Quantum Griffiths phase near an antiferromagnetic quantum critical point: Muon spin relaxation study of $Ce(Cu_{1-x}Co_x)_2Ge_2$

Rajesh Tripathi,[1] Debarchan Das,[1,2] P. K. Biswas,[3] D. T. Adroja,[3,4] A. D. Hillier,[3] and Z. Hossain[1,*]

[1]*Department of Physics, Indian Institute of Technology, Kanpur 208016, India*

[2]*Institute of Low Temperature and Structure Research, Polish Academy of Sciences, P.O. Box 1410, 50-950 Wrocław, Poland*

[3]*ISIS Facility, Rutherford Appleton Laboratory, Chilton, Didcot Oxon, OX11 0QX, United Kingdom*

[4]*Highly Correlated Matter Research Group, Physics Department, University of Johannesburg, P.O. Box 524, Auckland Park 2006, South Africa*

(Received 25 February 2019; revised manuscript received 3 June 2019; published 17 June 2019)

The antiferromagnetic order in the heavy-fermion compound $CeCu_2Ge_2$ can be suppressed by Co-doping, and at critical composition $x_c = 0.6$ ($T_N \to 0$ K) a quantum critical point has been observed. We have performed zero-field (ZF) and longitudinal-field muon spin relaxation (μSR) measurements on polycrystalline samples of $Ce(Cu_{1-x}Co_x)_2Ge_2$ ($x = 0, 0.2, 0.6, 1$) over a temperature range of 100 mK to 10 K and in applied fields from 0 up to 3000 G. Above any ordering temperature, the muon relaxation spectra can be described by a Gaussian-Kubo-Toyabe times exponential line shape. Below the magnetic ordering temperature (i.e., for $x < 0.6$), an additional Gaussian relaxation is observed. The zero-field muon relaxation rate suggests the presence of antiferromagnetic ordering below 4 and 0.8 K for $x = 0$ and 0.2 samples, respectively. For $x = 0.6$, the magnetic order is completely suppressed, and the quantum critical point is accompanied by non-Fermi-liquid behavior, manifested in the power-law divergence of exponential depolarization, i.e., $\lambda \propto T^{0.55}$. The relaxation rate of $x = 0.6$ obeys the time-field scaling relation $G_z(t, H) = G_z(t/H^{\gamma})$, which is considered to be a characteristic feature of quantum critical magnetic fluctuations. Furthermore, for $x = 0.6$, the exponent of isotherm magnetization, $M \sim H^{\eta}$, and magnetization-field-temperature scaling is consistent with the ZF-μSR data. These results provide strong evidence for the formation of a quantum Griffiths phase near the antiferromagnetic quantum phase transition.

DOI: 10.1103/PhysRevB.99.224424

I. INTRODUCTION

Quantum phase transitions (QPTs) have become one of the most fascinating areas of research in modern condensed-matter physics. They can be tuned by external parameters such as pressure, magnetic fields, or doping, from magnetically ordered to paramagnetic states as $T \to 0$ K. A quantum critical point (QCP) is expected to appear at the phase boundary and is characterized by a continuous development of the order parameter from zero in the paramagnetic state to nonzero in the ordered phase. In the vicinity of a QCP, many exotic phenomena have been observed, such as unconventional superconductivity [1–7], heavy-fermion (HF) behavior [6,8], and a breakdown of Landau Fermi-liquid behavior [called non-Fermi-liquid (NFL) behavior] [3,4,9]. Despite continuous efforts over the last two decades, the microscopic origin of the emergence of a NFL ground state is still not well understood. The single-ion multichannel Kondo effect, proximity to a $T \to 0$ K QCP, and the Kondo disorder model are among theoretical models proposed for NFL [3,4,10–14]. In addition, the NFL behavior of some chemically substituted f-electron systems is better described in the context of Castro-Neto theory based on Griffiths singularities [4,15–19]. These quantum Griffiths singularities can be attributed to rare magnetic regions embedded in the paramagnetic bulk [20,21]. Griffiths singularities also exist inside the long-range ordered magnetic phase [18,22]. At the QCP, NFL behavior in such systems is characterized by a power-law dependence of specific heat $C(T)/T \propto T^{-1+\eta}$, susceptibility $\chi(T) \propto T^{-1+\eta}$, and magnetization $M \propto H^{\eta}$, where η is slightly smaller than 1.0 [4,19,23,24]. Also, close to the critical concentration, all $M(H, T)$ data collapse on each other within a certain temperature range, which confirms non-single-impurity interpretation of the NFL behavior [25]. Understanding the origin of this NFL behavior near a QCP has become a stimulating area of research in strongly correlated d- and f-electron systems [26–30]. Since the dynamics of the spin fluctuations plays an essential role in the formation of magnetic clusters near a QCP and is responsible for NFL behavior, it is imperative to accumulate experimental information on the spin dynamics of disordered magnetic materials. The μSR technique is a very useful probe for characterizing unconventional magnetism, e.g., in heavy-fermion compounds [31], spin glasses [32], and disordered NFL metals [33], due to its extreme sensitivity to small magnetic fields (down to about 0.1 G), and therefore it can probe local magnetic fields that may be nuclear or electronic in origin.

Recently, we have investigated the system $Ce(Cu_{1-x}Co_x)_2Ge_2$, which has an interesting magnetic-phase

*zakir@iitk.ac.in

diagram where T_N shows two different slopes for $0 \leqslant x < 0.1$ and $0.1 \leqslant x < 0.6$ [34]. Moreover, NFL behavior develops for $x \sim 0.6$ as $T_N \to 0$ K. This feature is characterized by the formation of magnetic clusters in a nonmagnetic background known as the Griffiths phase. Here, we have carried out μSR measurements for $x = 0$, 0.2, 0.6, and 1 in order to gain further insight into the unusual magnetic ground state as well as the nature of low-energy spin fluctuations in the $x = 0.6$ sample. Our μSR experiment shows that the samples with $x = 0$ and 0.2 order magnetically below $T_N = 4$ and 0.8 K, respectively, which is in agreement with the macroscopic measurements such as magnetic susceptibility and specific heat. A power-law divergence of the μSR depolarization rate λ at low temperatures has been observed without any clear sign of magnetic ordering down to 100 mK for the $x = 0.6$ sample. Moreover, our study confirms the presence of a quantum Griffiths phase in $x = 0.6$.

II. EXPERIMENTAL DETAILS

Polycrystalline samples of $Ce(Cu_{1-x}Co_x)_2Ge_2$ for $0 \leqslant x \leqslant 1$ were prepared by arc melting of the constituent elements in an argon atmosphere. Samples were subjected to a heat treatment in evacuated sealed quartz tubes at 850 °C for one week. Powder x-ray diffraction with Cu $K\alpha$ radiation at room temperature was used to determine the phase purity and crystal structure. The magnetic measurements were performed using a commercial vibrating sample magnetometer (VSM) attached with the physical property measurement system (PPMS, Quantum Design). Muon spin relaxation measurements were performed using the μSR spectrometer at the ISIS facility, Rutherford Appleton Laboratory, Didcot, UK [35], both in zero field and in longitudinal fields up to 3000 G. For these measurements, the powder samples of $Ce(Cu_{1-x}Co_x)_2Ge_2$ for $x = 0$, 0.2, 0.6, and 1 were mounted on high-purity silver plates using diluted GE varnish and covered with a thin silver foil. A sample temperature down to 100 mK was achieved using a dilution refrigerator. The ZF-μSR spectra were recorded at several temperatures between 100 mK to 10 K, and LF data were collected at temperatures well above and below magnetic ordering temperature for fields between 0 and 3000 G. In the μSR measurement, spin-polarized muons (μ^+) are implanted into the sample, after which they decay into a positron e^+ and two neutrinos ν_e, $\bar{\nu_\mu}$ with an average lifetime τ_μ of 2.2 μs and they are emitted preferentially in the direction of the muon spin axis. When muons are subjected to magnetic interactions in a sample, their asymmetry evolves with time. The asymmetry function, $G_z(t)$, is determined by measuring the distribution of emitted e^+ in the forward and backward directions with respect to the initial μ^+ momentum by the detectors that are positioned before (F) and after (B) the sample. The asymmetry function is defined as $G_z(t) = [N_F(t) - \alpha N_B(t)]/[N_F(t) + \alpha N_B(t)]$, where $N_F(t)$ and $N_B(t)$ are the number of muon events counted by the forward and backward detectors at time t, respectively, and α is a calibration constant that reflects the relative counting efficiency of the forward and backward counters and is determined from calibration measurements made in the paramagnetic state with a small applied transverse magnetic field of 20 G. $G_z(t)$ provides information about the internal field and the spin lattice relaxation rate.

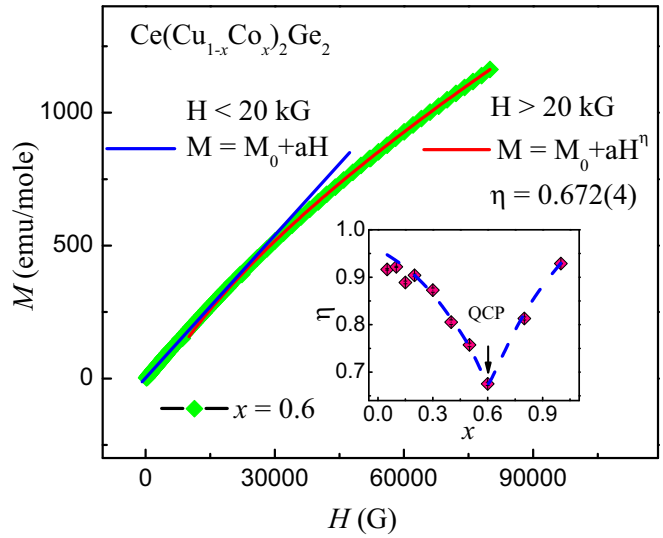

FIG. 1. Magnetization as a function of field at $T = 2.5$ K for $x = 0.6$, showing a linear behavior, $M \sim H$, for $H < 20$ kG and a power-law behavior, $M \sim H^\eta$, for $H > 20$ kG. The inset shows nonuniversal exponent η vs x.

III. RESULTS AND DISCUSSION

A. Magnetic characterization

Recently, we have reported that the NFL system $Ce(Cu_{1-x}Co_x)_2Ge_2$ follows power-law behavior for $x = 0.6$ both in $C(T)/T$ and $\chi(T)$ based on a Griffiths phase scenario [34]. To further characterize $Ce(Cu_{0.4}Co_{0.6})_2Ge_2$ and to better determine whether a quantum Griffiths phase scenario applies best, the magnetization was measured as a function of magnetic field, as shown in Fig. 1. The magnetization follows the predicted Griffiths phase behavior $M(H) = M_0 + aH^\eta$, where M_0 is the negative constant offset and η is the same as in the temperature dependence of χ, above some crossover field of about 20 kG up to the highest available field of 80 kG [22,36]. However, the power-law dependency breaks down below this crossover field of 20 kG, and the magnetization behaves as $M \sim H$. The best fit yields the exponent $\eta = 0.672(4)$, which is consistent with the value determined from $C(T)/T$ and $\chi(T)$ in our previous report [34]. The inset of Fig. 1 shows the variation of exponent η with concentrations x on both sides of the QPT at $T = 2.5$ K (i.e., in the paramagnetic regime). The exponent η is nonuniversal, i.e., strongly x-dependent. It has a minimum close to the critical concentration x_c and increases monotonically with increasing distance from x_c. It should be noted that a similar kind of behavior has also been observed for ferromagnetic systems like $Ni_{1-x}V_x$, where the M versus H isotherms have been measured below the ordering temperature for $x < x_c$ and attributed to the presence of magnetic clusters in the paramagnetic bulk [22]. Also, our magnetization data are consistent with the scaling behavior found in systems like $U(Cu, Pd)_5$, $U_{1-x}Y_xPd_3$, $Ce_{1-x}Th_xRhSb$, $CePd_{1-x}Rh_x$ [25,37–39], and is described by

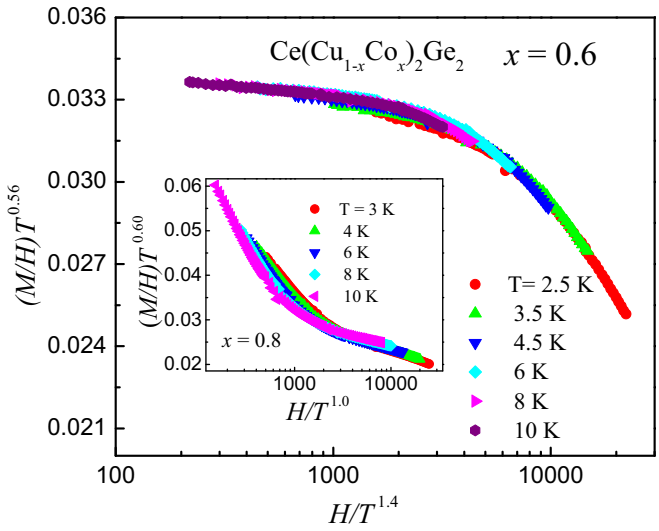

FIG. 2. The magnetization $(M/H)T^{0.56}$ vs $\log(H/T^{1.4})$ for $x = 0.6$ and 0.8 (inset). M is expressed in emu/mole, H in G, and T in K.

the following functional form:

$$\frac{M}{H} = T^{-\eta_m} \times g\left(\frac{H}{T^{\beta_m}}\right). \tag{1}$$

Here we used subscript m just to avoid confusion with the symbols used in the muon relaxation function. The corresponding scaling plot for $x = 0.6$ is shown in the main panel of Fig. 2. All the $M(H, T)$ curves in the temperature range 2.5–10 K are superimposed on each other, confirming the $M(H, T)$ scaling. We have produced similar scaling plots for $x = 0.8$ (see the inset of Fig. 2). The scaling for $x = 0.8$ is less perfect than the scaling for $x = 0.6$. The resulting value of the exponent $\eta = 0.56(2)$ nearly matches with that obtained by a direct fit of the power law for $x = 0.6$. In addition, the magnetic-field scaling exponent (β_m) is nearly equal to 1.4 for $x = 0.6$. The scaling dimension greater than 1 is an indication of the non-single-impurity interpretation of NFL behavior near the quantum critical point and ruling out single-ion theories, which have scaling dimension less than 1 [25]. We emphasize that no such scaling behavior should be observed for a FL system. The value of the magnetic-field scaling exponent $(\beta_m > 1)$ implies non-single-impurity interpretation of the NFL behavior of $Ce(Cu_{0.4}Co_{0.6})_2Ge_2$. The presence of $M(H, T)$ scaling also indicates that the system has a second-order phase transition at $T = 0$ [25], consistent with our previous claim based on the magnetic phase diagram. This value of η_m is comparable with the exponent obtained from the temperature dependence of the spin relaxation rate, presented in the next section.

B. μSR measurements

In this section, in order to understand the magnetic interactions on a microscopic level, we presented μSR measurements of $Ce(Cu_{1-x}Co_x)_2Ge_2$ for $x = 0$, 0.2, 0.6, and 1. The results confirm the development of an inhomogeneous local magnetic field below the ordering temperature, with a nearly full volume fraction for $x = 0$ and a diminishing volume fraction as a function of doping concentration, x. The μSR data clearly rule out any possible static magnetic ordering for $x = 0.6$ and 1. Moreover, we find that the critical exponent determined from the power-law behavior of $M(H)$ as well as scaling analysis of the $M(H, T)$ for $x = 0.6$ is consistent with the μSR results.

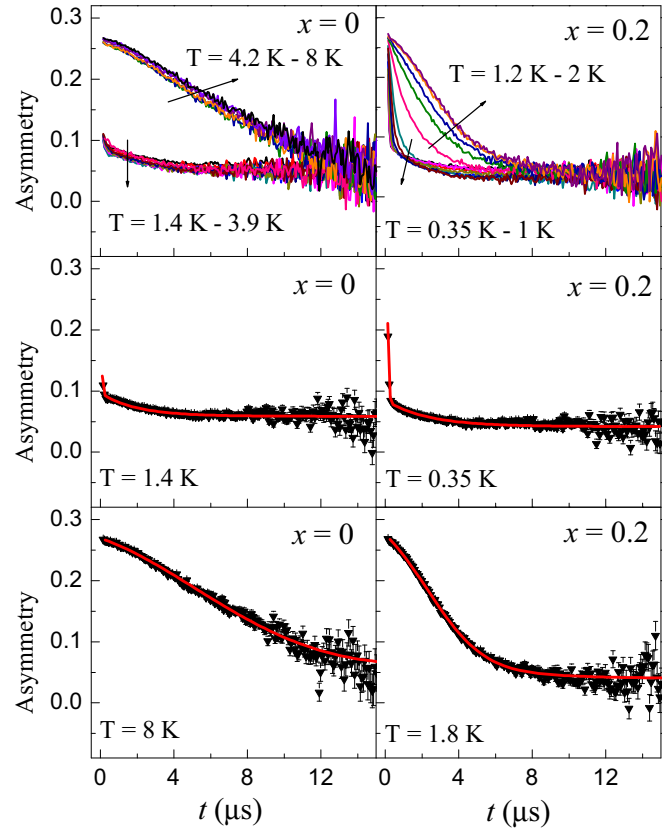

FIG. 3. ZF-μSR time spectra of $Ce(Cu_{1-x}Co_x)_2Ge_2$ for $x = 0$ and 0.2 measured at different temperatures. The solid lines represent fits to the relaxation functions given by Eq. (2).

1. *ZF- and LF-μSR spectra for* $Ce(Cu_{1-x}Co_x)_2Ge_2$ ($x = 0, 0.2$)

Figure 3 shows the time dependence of ZF-μSR asymmetry spectra collected on $Ce(Cu_{1-x}Co_x)_2Ge_2$ for $x = 0$ and 0.2 samples, measured at various temperatures. While for $x = 0$ we observe a drastic change in μSR spectra at $T = 4$ K for $x = 0.2$, the change at $T = 0.8$ K is broader than expected, which might be due to the distribution of T_N values in the $x = 0.2$ sample. We do not see a clear oscillation in the ordered state of the μSR spectra in $x = 0$ or 0.2 related to the muon spin precession. In contrast, clear oscillations are observed below T_N in $Ce(Cu_{1-x}Ni_x)_2Ge_2$ for $x = 0$ and 0.1 [40], where the measurements have been performed at TRIUMF, Vancouver. The absence of oscillations below ordering temperature in our case is due to a pulse width (70 ns) of muon beam at ISIS, which does not allow us to collect data very close to zero time, which is very important for the materials having ordering with large ordered state moments. The data for $x = 0$ and 0.2 have been successfully fitted to the muon

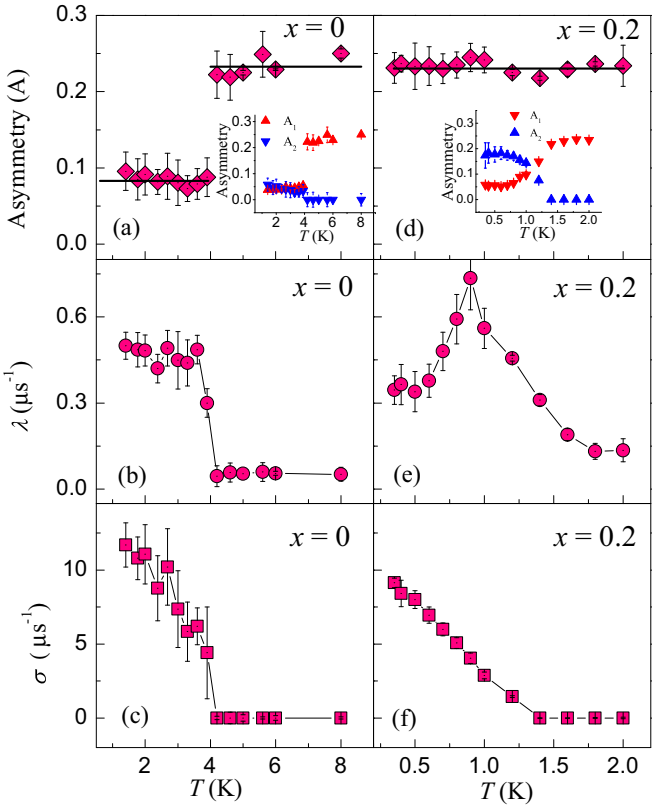

FIG. 4. Temperature dependence of the effective initial asymmetry ($A = A_1 + A_2$), depolarization rate λ and σ for $x = 0$ and 0.2, obtained from the fitting of the μSR spectra using Eq. (2). The insets of (a) and (d) show the asymmetry of slow exponential component (A_1) and fast Gaussian component (A_2) for $x = 0$ and 0.2, respectively.

spin relaxation function described in Eq. (2),

$$G_z(t) = G_{\mathrm{KT}}(t)\left[A_1\exp(-\lambda t) + A_2\exp\left(\frac{-\sigma^2 t^2}{2}\right)\right] + A_{\mathrm{BG}}, \quad (2)$$

where $A = A_1 + A_2$ represents the effective initial asymmetry of the signal, and λ and σ are the depolarization rates. A_{BG} is a constant background arising from muon stopping on the silver sample holder. The static Kubo-Toyabe function

$$G_{\mathrm{KT}}(t) = \frac{1}{3} + \frac{2}{3}[1 - (\sigma_{\mathrm{KT}}t)^2]\exp\left(\frac{-\sigma_{\mathrm{KT}}^2 t^2}{2}\right) \quad (3)$$

describes the muon spin depolarization with a rate of σ_{KT} caused by randomly oriented ^{63,65}Cu, ^{59}Co, and ^{73}Ge nuclei. Best fits to the spectra yielded $\sigma_{\mathrm{KT}} = 0.09(2)$ and 0.12(3) μs^{-1} above the ordering temperature and equal to zero below the ordering temperature for $x = 0$ and 0.2, respectively. The first exponential component in Eq. (2) accounts for dynamic magnetic fluctuations, whereas the second term describes the Gaussian distribution of static fields. The need for a broad field distribution (Gaussian) to describe the antiferromagnetic component indicates a strongly inhomogeneous order. The fitting parameters, determined from the best fits, are displayed in Fig. 4. The temperature dependence of the initial asymmetry

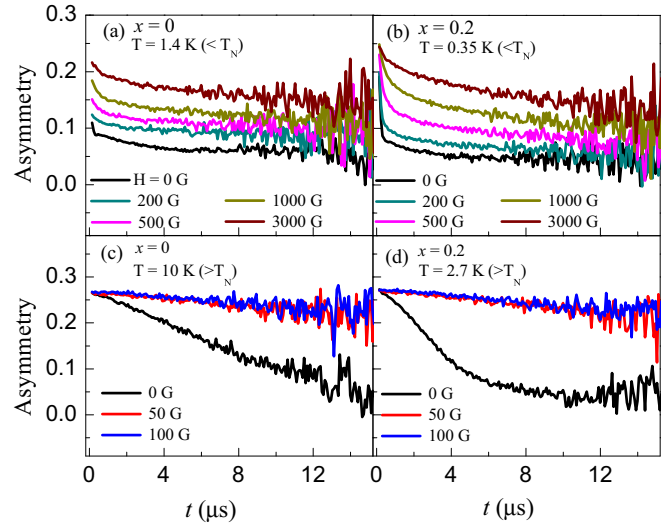

FIG. 5. LF-μSR time spectra of $Ce(Cu_{1-x}Co_x)_2Ge_2$ for $x = 0$ and 0.2 above and below ordering temperature at different field up to 3000 G.

for $x = 0$ and 0.2 is presented in Figs. 4(a) and 4(d), respectively. For $x = 0$, the effective initial asymmetry (A) exhibits a nearly 1/3 drop below 4 K [Fig. 4(a)], indicating that the long-range magnetic ordering occurs in the full volume of the sample and hence has a bulk nature. For $x = 0.2$, we do not observe any significant change in effective initial asymmetry [Fig. 4(d)]. However, A_1 and A_2 independently show significant changes around $T = 0.8$ K [inset of Fig. 4(d)]. This is near the temperature where C/T and $\chi(T)$ show a maximum. As the transition T_N is approached, λ [see Figs. 4(b) and 4(e)] shows an increase with decreasing temperature. The enhancement of λ indicates a slowing down of Ce spin fluctuations due to the development of strong correlations, a common feature seen in other AFM and FM materials below magnetic ordering temperature [18,22,41]. Furthermore, with the lowering of temperature, below magnetic ordering, λ levels off for $x = 0$ [Fig. 4(b)] whereas it decreases drastically for $x = 0.2$ [Fig. 4(e)]. The possible mechanism leading to the reduction of λ below T_N could be that the fluctuations are static in nature, as seen in the increase in the σ in Fig. 4(f). The damping rate σ, which reflects the width of the local field distribution at the muon site, is displayed in Figs. 4(c) and 4(f) for $x = 0$ and 0.2, respectively. An increase below 4 K and about 1.5 K is observed in the temperature dependence of σ for $x = 0$ and 0.2, respectively, while it is almost temperature-independent above the mentioned temperatures. The two-component μSR signal observed in $Ce(Cu_{1-x}Co_x)_2Ge_2$ has also been found in several other rare-earth heavy-fermion compounds, such as $CeCu_2Si_2$, YbBiPt, $CeAl_3$, $CeRh_2Si_2$, $CeCoGe_{3-x}Si_x$, and CeRhBi [18,31,42–45].

Figure 5 shows μSR asymmetry data well above and below magnetic ordering temperature in the longitudinal external field of 0–3000 G for $x = 0$ and 0.2 samples. A small longitudinal field can suppress muon spin depolarization caused by weaker local static fields, typically due to nuclear dipole moments, whereas depolarization due to fast fluctuating local fields (in our case Ce $4f$ spins) may only be affected by

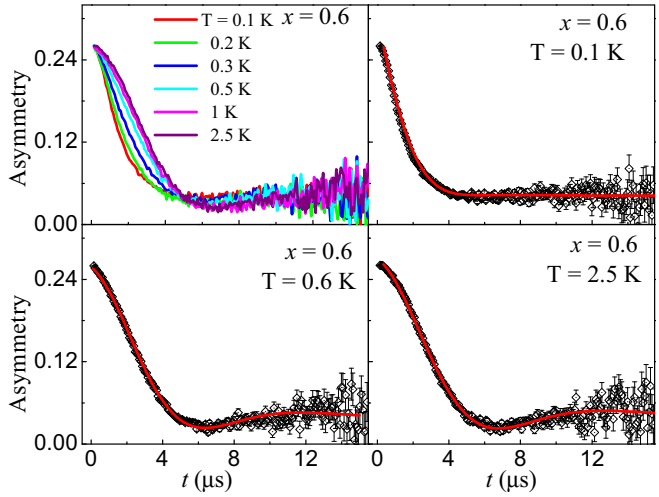

FIG. 6. ZF-μSR spectra of $Ce(Cu_{0.4}Co_{0.6})_2Ge_2$ in the temperature range 0.1 to 2.5 K. The solid lines represent fits to the relaxation functions given by Eq. (4).

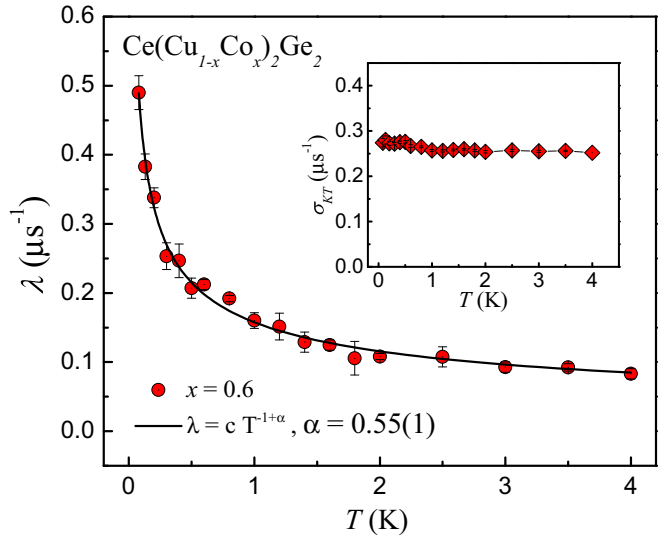

FIG. 7. Temperature dependence of relaxation rate λ obtained from the fitting of the μSR spectra using Eq. (4). The solid line represents power-law behavior of λ. The inset shows the temperature dependence of nuclear depolarization rate σ_{KT} in the given temperature range.

much larger applied fields. It is clear from the LF spectra in Fig. 5 that a 50 G LF is enough for almost complete suppression of the depolarization above ordering temperature [Figs. 5(c) and 5(d)] for both $x = 0$ and 0.2 samples. However, below the ordering temperature, the muon depolarization is gradually reduced by much higher fields [Figs. 5(a) and 5(b)] and is not suppressed completely even with an applied LF of 3000 G. This indicates that the observed relaxation is due to a static field, generated by the static magnetic order in both the undoped and doped systems.

2. *ZF- and LF-μSR spectra for* $Ce(Cu_{1-x}Co_x)_2Ge_2$ ($x = 0.6, 1$)

The ZF-μSR spectra at various temperatures between 100 mK and 4 K in $Ce(Cu_{0.4}Co_{0.6})_2Ge_2$ are shown in Fig. 6, which can be best fitted by Eq. (4) given below:

$$G_z(t) = A_0 G_{KT}(t) \times \exp(-\lambda t) + A_{BG}, \quad (4)$$

where A_0 is the initial asymmetry. The A_{BG} was estimated from 2 K data and was kept fixed for fitting all the other spectra. The value of σ_{KT} was found to be $\sim$0.27(4) μs^{-1} from fitting the spectra above 2.5 K, and this value was found to be nearly temperature-independent down to 100 mK. The values of the parameters σ_{KT} and λ, estimated from our analysis, are plotted in Fig. 7 as a function of temperature. We have not observed any signature of static magnetic ordering in the μSR experiments in $Ce(Cu_{0.4}Co_{0.6})_2Ge_2$ down to 100 mK. It can be seen from Fig. 7 that λ exhibits a power-law-type behavior with an exponent $\alpha = 0.55(1)$. This exponent value is in excellent agreement with the values 0.66 and 0.53 obtained from the temperature dependence of the magnetic susceptibility and $C(T)/T$ of $Ce(Cu_{0.4}Co_{0.6})_2Ge_2$, respectively [34], as well as with the value of $\eta = 0.56(2)$ obtained from magnetization scaling, as mentioned previously. This agreement is a strong indication for the coexistence of uncorrelated local moments as short-range-ordered spin clusters in the paramagnetic environment and is clear evidence for the formation of a Griffiths phase in $Ce(Cu_{0.4}Co_{0.6})_2Ge_2$. Also, our data do not follow the typical relaxation function reported for a spin-glass system [32].

To further study the role of static and dynamic local internal fields and to investigate the time-field scaling, we have carried out μSR measurements in applied longitudinal fields between 0 and 3000 G at 0.1 K (main panel of Fig. 8) and at 4 K (inset of Fig. 8). The muon spin relaxation in longitudinal fields is mainly due to spin fluctuations of $4f$ moments, which are coupled with the muons implanted in the sample. Due to the spin fluctuations of the neighboring $4f$ moments, these muons at a given site experience a time-varying local internal field $H_{loc}(t)$. Although the Griffiths

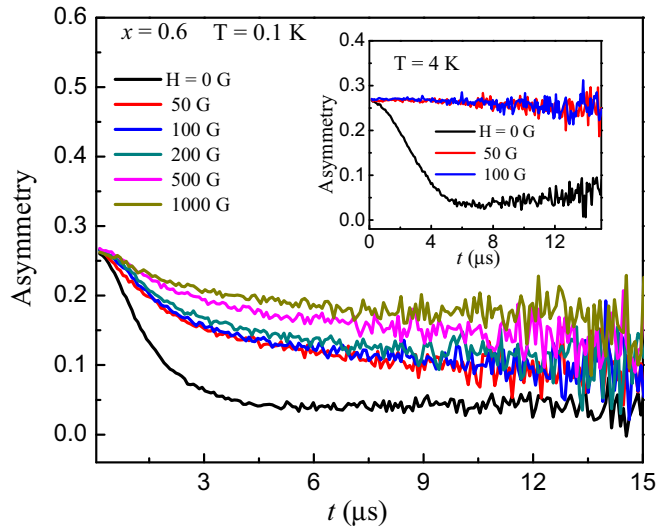

FIG. 8. LF-μSR spectra of $Ce(Cu_{0.4}Co_{0.6})_2Ge_2$ at $T = 100$ mK in the different field up to 1000 G. The inset shows LF-μSR spectra at $T = 4$ K in the applied field up to 100 G.

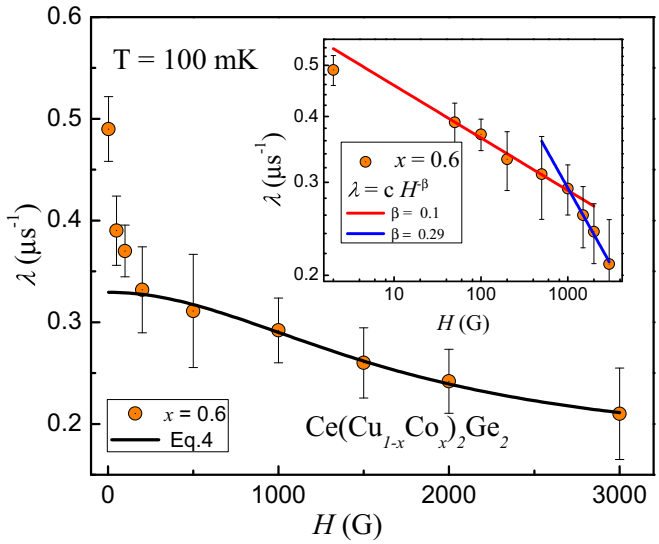

FIG. 9. LF dependence of the relaxation rate λ. It may be noted that the lower field changes could arise from the decoupling of muons with the nuclear moments. The solid lines indicate the fit results obtained with Eq. (5). The inset shows the log-log plot with the solid lines representing power-law behaviors with different exponents.

phase mechanism has been considered as a promising theory for explaining the NFL behavior in this system [34], investigation of low-temperature muon spin dynamics is expected to provide additional information about the origin of NFL behavior in $Ce(Cu_{0.4}Co_{0.6})_2Ge_2$. In the following, we discuss the field and temperature dependence of the relaxation rate of the muon spin obtained from LF-μSR experiments.

Under the influence of an external magnetic field H_{LF}, parallel to the initial muon polarization, muons decouple themselves from the static and dynamics fluctuations, and hence the muon relaxation rate is expected to decrease with the applied longitudinal field. It is clear from Fig. 9 that initially

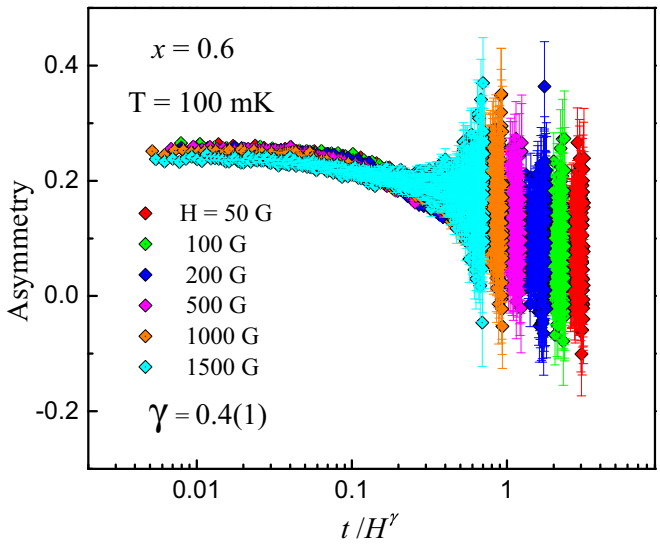

FIG. 10. Time-field scaling of the μSR relaxation function, $G_z(t)$ vs (t/H^{γ}), for $Ce(Cu_{0.4}Co_{0.6})_2Ge_2$ at 100 mK.

λ decreases very fast followed by a weak field dependence up to $H = 3000$ G. The spin autocorrelation time τ_c can also be estimated from the longitudinal-field dependence of λ. We use $\lambda(H)$ data of $x = 0.6$ measured at $T = 100$ mK, shown in Fig. 9, to estimate the spin autocorrelation time τ_c of spin fluctuation using the following Redfield equation [32]:

$$\lambda = \lambda_0 + \frac{2\gamma_\mu^2\langle H_{\rm loc}^2\rangle\tau_c}{1+\gamma_\mu^2 H_{\rm LF}^2\tau_c^2}, \tag{5}$$

where λ_0 is the H-independent depolarization rate and $H_{\rm loc}$ is the time average of the second moment of the time-varying local field $H_{\rm loc}(t)$ at muon sites due to the fluctuations of neighboring Ce $4f$ moments. The internal field has been determined by measuring the longitudinal field (LF) dependence of muon spin relaxation rates at 100 mK. The best fit to λ by Eq. (5), shown by the solid curve in Fig. 9, returned the fitting parameters $\lambda(0) = 0.17$ μs, $\langle H_{\rm loc}\rangle = 40(8)$ G, and $\tau_c = 68$ ns. A correlation time of about 37 and 42 ns was found in $CeCoGe_{1.8}Si_{1.2}$ and stoichiometric CeRhBi, respectively [18,45]. The value of τ_c in $Ce(Cu_{0.4}Co_{0.6})_2Ge_2$ is much larger compared to the typical range of 0.10–0.01 ns observed in metallic spin glasses such as CuMn [32] and usually comes from disordered spin arrangements. Long correlation times (slow magnetic fluctuations) are generally expected in the critical region just above a magnetic transition. To illustrate the behavior of λ with H, we plotted λ versus H on a log-log scale, shown in the inset of Fig. 9. A power-law behavior, $\lambda \sim H^{-\beta}$, with $\beta = 0.10(1)$ in the low-field regime and $\beta = 0.29(1)$ in the high-field regime, can be found from this analysis. The observation of two scaling exponents in field dependence λ is quite unique in the existing literature (see Ref. [39]). We anticipate that this change in the exponent is due to the dimensional crossover of critical fluctuations (from 2D AFM to 3D AFM fluctuations). Such dimensional crossover of critical fluctuations may occur while tuning either the temperature or the nonthermal tuning parameter (in this case applied field) [46]. Further detailed investigation such as inelastic neutron scattering will be worthwhile to address this tempting issue. This behavior is further evidence for a long correlation time at the muon stopping site, which is considered to be a characteristic feature of quantum critical magnetic fluctuations. It is interesting to compare these values with $CeRu_4Sn_6$, exhibiting NFL behavior with a spin gap, which has a value of $\beta = 0.17$ [47].

Furthermore, we find that the LF-μSR data follow characteristic time-field scaling $G_z(t, H) = G_z(t/H^{\gamma})$, where the exponent γ provides information about spin-spin dynamical autocorrelation [33,48]. Time-field scaling is a signature of slow dynamics and has been observed for both classical spin-glass systems and NFL systems having local f moments. The time-field scaling can, in principle, appear near any critical point but is usually associated with spin-glass-like behavior [33]. For systems with NFL behavior, such glassy spin dynamics can result from the effect of disorder on critical quantum fluctuations. By observing the time-field scaling, independent information on the nature of the spin autocorrelation function $q(t)$ can be obtained. It is also to be noted that $q(t)$ is theoretically predicted to exhibit a power law or stretched exponential behavior with $\gamma < 1$ for power-law correlation

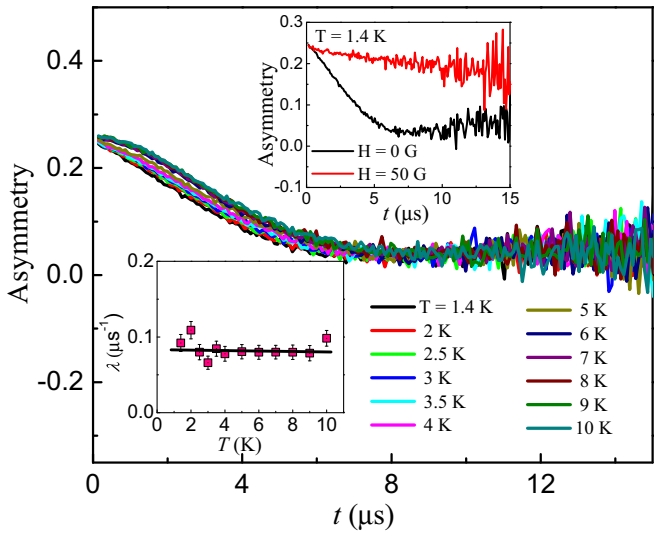

FIG. 11. ZF-μSR time spectra of $CeCo_2Ge_2$ measured at different temperatures. The upper inset shows LF-μSR spectra up to 50 G, whereas the lower inset shows the temperature dependence of relaxation rate λ obtained from the fitting of the μSR spectra using Eq. (4)

and $\gamma > 1$ for stretched exponential correlation [33,49]. The asymmetry as a function of scaling variable t/H^{γ} for $x = 0.6$ is plotted between 50 and 1500 G at 0.1 K in Fig. 10. Similar time-field scaling has also been observed in $UCu_{5-x}Pd_x$, $CePtSi_{1-x}Ge_x$, $CePd_{0.15}Rh_{0.85}$, CeRhBi [33,39,45,48], as well as of the spin-glass system AgMn (0.5 at. % Mn) above T_g [50]. The best scaling of the overall data can be obtained with $\gamma = 0.4(1)$, except for the high-field data with 1500 G field, which show considerable deviation from the scaling curve. A time-field scaling breakdown would occur for high fields indicating that the applied fields directly affect $q(t)$. A similar kind of deviation has also been found in $YbNi_4P_2$ around the ferromagnetic quantum critical point but at a very low applied field of 300 G [51]. The observed value of $\gamma = 0.4$ for $Ce(Cu_{0.4}Co_{0.6})_2Ge_2$ is very similar to the value observed for UCu_4Pd ($\gamma = 0.35$) but smaller than the values observed for $UCu_{3.5}Pd_{1.5}$, CePtBi ($\gamma = 0.7, 0.8$), and $CePtSi_{1-x}Ge_x$ ($\gamma = 1.6$ for $x = 0$ and 0.1). A value of $\gamma = 1/2$ is also predicted by the mean-field model of a disordered Kondo alloy at a quantum critical point [52]. The scaling exponent γ is less than 1, implying that the spin autocorrelation function $q(t)$ is well approximated by a power law rather than a stretched exponential or exponential ($\gamma > 1$) [33]. Therefore, it would be interesting to investigate directly the form of $q(t)$ using a neutron spin-echo technique for $Ce(Cu_{0.4}Co_{0.6})_2Ge_2$. The main panel of Fig. 11 shows ZF μSR spectra of valance fluctuating $CeCo_2Ge_2$ [53], measured at temperatures between 1.4 and 10 K, which could be best fitted by Eq. (4), yielding a nearly constant value of $\lambda = 0.1\ \mu s^{-1}$ (see the lower inset of Fig. 11), consistent with the paramagnetic fluctuation of Ce moments. The LF spectra in the upper inset of Fig. 11 show that these fluctuations are completely suppressed by a small applied LF of 50 G.

IV. CONCLUSION

In conclusion, we have performed ZF- and LF-μSR experiments on a heavy-fermion system $Ce(Cu_{1-x}Co_x)_2Ge_2$ for $x = 0$, 0.2, 0.6, and 1. The ZF-μSR data confirm the magnetic ordering below $T_N = 4$ and 0.8 K for $x = 0$ and 0.2 samples, respectively. We found that the temperature dependence of the ZF-μSR dynamic relaxation rate λ, close to critical concentration $x_c = 0.6$, exhibits a power-law behavior, $\lambda \sim T^{-\alpha}$, with an exponent $\alpha = 0.55(1)$, attributed to the existence of magnetic clusters at low temperature in the quantum critical regime. The observed value of the exponent α is in good agreement with exponents $\eta_m = 0.56(2)$ and $\eta = 0.67$, obtained from magnetization-field-temperature scaling and the power-law Griffiths singularity, $M \sim H^{\eta}$, respectively, which provides further evidence of the presence of such clusters inside a paramagnetic environment. Furthermore, the LF-μSR data for $x = 0.6$ at 100 mK exhibit a time-field scaling with the exponent $\gamma = 0.4(1)$, which suggests that the spin-spin autocorrelation function has a power-law behavior. The large value of the spin autocorrelation time τ_c, even larger than that for spin-glass systems, is again indicative of disorder-induced NFL behavior. These results show that around the quantum phase transition (at $x = 0.6$), the Griffiths phase crucially controls the low-temperature spin dynamics and is responsible for NFL behavior.

ACKNOWLEDGMENTS

We would like to thank the Science and Technology Facility Council (STFC), Rutherford Appleton Laboratory (RAL) for allocation of μSR beam time (RB1768032) under India-access. Travel support for R.T. and Z.H. was provided by the Newton-India fund and the India-RAL project in neutron and muon, respectively.

[1] B. Keimer, S. A. Kivelson, M. R. Norman, S. Uchida, and J. Zaanen, Nature (London) **518**, 179 (2015).
[2] Y. J. Uemura, Nat. Mater. **8**, 253 (2009).
[3] G. R. Stewart, Rev. Mod. Phys. **73**, 797 (2001).
[4] H. V. L öhneysen, A. Rosch, M. Vojta, and P. Wölfle, Rev. Mod. Phys. **79**, 1015 (2007).
[5] P. Gegenwart, Q. Si, and F. Steglich, Nat. Phys. **4**, 186 (2008).
[6] C. Pfleiderer, Rev. Mod. Phys. **81**, 1551 (2009).
[7] M. Brando, D. Belitz, F. M. Grosche, and T. R. Kirkpatrick, Rev. Mod. Phys. **88**, 025006 (2016).
[8] N. D. Mathur, F. M. Grosche, S. R. Julian, I. R. Walker, D. M. Freye, R. K. W. Haselwimmer, and G. G. Lonzarich, Nature (London) **394**, 39 (1994).
[9] G. Sparn, M. Deppe, L. Donnevert, C. Geibel, P. Hellmann, K. Heuser, M. Koeppen, M. Lang, F. Laube, A. Link, S. Thomas, and F. Steglich, Physica B **230**, 317 (1997).
[10] G. R. Stewart, Rev. Mod. Phys. **78**, 743 (2006).
[11] Q. Si, S. Rabello, K. Ingersent, and J. L. Smith, Nature (London) **413**, 804 (2001).

[12] P. Coleman, C. P épin, Q. Si, and R. Ramazashvili, J. Phys.: Condens. Matter **13**, R723 (2001).

[13] Q. Si, J. H. Pixley, E. Nica, S. J. Yamamoto, P. Goswami, R. Yu, and S. Kirchner, J. Phys. Soc. Jpn. **83**, 061005 (2014).

[14] E. Miranda and V. Dobrosavljevic, Rep. Prog. Phys. **68**, 2337 (2005).

[15] K. Ghosh, C. Mazumdar, R. Ranganathan, and S. Mukherjee, Sci. Rep. **5**, 15801 (2015).

[16] Y. Lai, S. E. Bone, S. Minasian, M. G. Ferrier, J. Lezama-Pacheco, V. Mocko, A. S. Ditter, S. A. Kozimor, G. T. Seidler, W. L. Nelson, Y.-C. Chiu, K. Huang, W. Potter, D. Graf, T. E. Albrecht-Schmitt, and R. E. Baumbach, Phys. Rev. B **97**, 224406 (2018).

[17] M. T. Tran and K. S. Kim, J. Phys.: Condens. Matter **23**, 425602 (2011).

[18] V. V. Krishnamurthy, K. Nagamine, I. Watanabe, K. Nishiyama, S. Ohira, M. Ishikawa, D. H. Eom, T. Ishikawa, and T. M. Briere, Phys. Rev. Lett. **88**, 046402 (2002).

[19] M. C. de Andrade, R. Chau, R. P. Dickey, N. R. Dilley, E. J. Freeman, D. A. Gajewski, M. B. Maple, R. Movshovich, A. H. Castro Neto, G. Castilla, and B. A. Jones, Phys. Rev. Lett. **81**, 5620 (1998).

[20] T. Vojta and J. Schmalian, Phys. Rev. B **72**, 045438 (2005).

[21] J. A. Hoyos, C. Kotabage, and T. Vojta, Phys. Rev. Lett. **99**, 230601 (2007); T. Vojta, C. Kotabage, and J. A. Hoyos, Phys. Rev. B **79**, 024401 (2009).

[22] R. Wang, A. Gebretsadik, S. Ubaid-Kassis, A. Schroeder, T. Vojta, P. J. Baker, F. L. Pratt, S. J. Blundell, T. Lancaster, I. Franke, J. S. Möller, and K. Page, Phys. Rev. Lett. **118**, 267202 (2017).

[23] A. H. Castro Neto, G. Castilla, and B. A. Jones, Phys. Rev. Lett. **81**, 3531 (1998).

[24] T. Vojta, J. Low Temp. Phys. **161**, 299 (2010).

[25] B. Andraka and A. M. Tsvelik, Phys. Rev. Lett. **67**, 2886 (1991).

[26] K. Heuser, E. W. Scheidt, T. Schreiner, and G. R. Stewart, Phys. Rev. B **57**, R4198 (1998).

[27] E. Bauer, R. Hauser, A. Galatanu, H. Michor, G. Hilscher, J. Sereni, M. G. Berisso, P. Pedrazzini, M. Galli, F. Marabelli, and P. Bonville, Phys. Rev. B **60**, 1238 (1999).

[28] E. Svanidze, T. Besara, J. K. Wang, D. Geiger, L. Prochaska, J. M. Santiago, J. W. Lynn, S. Paschen, T. Siegrist, and E. Morosan, Phys. Rev. B **95**, 220405(R) (2017).

[29] A. Loidl, A. Krimmel, K. Knorr, G. Sparn, M. Lang, C. Geibel, S. Horn, A. Grauel, F. Steglich, B. Welslau, N. Grewe, H. Nakotte, F. R. de Boer, and A. P. Murani, Ann. Phys. **504**, 78 (1992).

[30] G. Sparn, R. Caspary, U. Gottwick, A. Grauel, U. Habel, M. Lang, M. Nowak, R. Schefzyk, W. Schiebeling, H. Spille, M. Winkelmann, A. Zuber, F. Steglich, and A. Loidl, J. Magn. Magn. Mater. **76-77**, 153 (1988).

[31] A. Amato, Rev. Mod. Phys. **69**, 1119 (1997).

[32] Y. J. Uemura, T. Yamazaki, D. R. Harshman, M. Senba, and E. J. Ansaldo, Phys. Rev. B **31**, 546 (1985).

[33] D. E. MacLaughlin, R. H. Heffner, O. O. Bernal, K. Ishida, J. E. Sonier, G. J. Nieuwenhuys, M. B. Maple, and G. R. Stewart, J. Phys.: Condens. Matter **16**, S4479 (2004).

[34] R. Tripathi, D. Das, C. Geibel, S. K. Dhar, and Z. Hossain, Phys. Rev. B **98**, 165136 (2018).

[35] Muon spin relaxation study of Co-doped $CeCu_2Ge_2$, doi: 10.5286/ISIS.E.90576407.

[36] A. H. Castro Neto and B. A. Jones, Phys. Rev. B **62**, 14975 (2000).

[37] A. M. Tsvelik and M. Reizer, Phys. Rev. B **48**, 9887 (1993).

[38] B. Andraka and G. R. Stewart, Phys. Rev. B **47**, 3208 (1993).

[39] D. T. Adroja, A. D. Hillier, J.-G. Park, W. Kockelmann, K. A. McEwen, B. D. Rainford, K.-H. Jang, C. Geibel, and T. Takabatake, Phys. Rev. B **78**, 014412 (2008).

[40] H. H. Klauss, M. A. C. de Melo, S. S¨llow, H. Walf, D. Mienert, D. Baabe, F. J. Litterst, and C. Geibel, Physica B **312-313**, 425 (2002).

[41] O. Mustonen, S. Vasala, E. Sadrollahi, K. P. Schmidt, C. Baines, H. C. Walker, I. Terasaki, F. J. Litterst, E. Baggio-Saitovitch, and M. Karppinen, Nat. Commun. **9**, 1085 (2018).

[42] A. Schenck and F. N. Gygax, in *Handbook of Magnetic Materials*, edited by K. H. J. Buschow (Elsevier, Amsterdam, 1995), Vol. 9, p. 57.

[43] V. K. Pecharsky, O. B. Hyun, and K. A. Gschneidner, Phys. Rev. B **47**, 11839 (1993).

[44] A. Amato, P. C. Canfield, R. Feyerherm, Z. Fisk, F. N. Gygax, R. H. Heffner, D. E. MacLaughlin, H. R. Ott, A. Schenck, and J. D. Thompson, Phys. Rev. B **46**, 3151 (1992).

[45] V. K. Anand, D. T. Adroja, A. D. Hillier, K. Shigetoh, T. Takabatake, J.-G. Park, K. A. McEwen, J. H. Pixley, and Q. Si, J. Phys. Soc. Jpn. **87**, 064708 (2018).

[46] M. Garst, L. Fritz, A. Rosch, and M. Vojta, Phys. Rev. B **78**, 235118 (2008).

[47] A. Strydom, A. D. Hillier, D. T. Adroja, S. Paschen, and F. Steglich, J. Magn. Magn. Mater. **310**, 377 (2007).

[48] O. O. Bernal, D. E. MacLaughlin, H. G. Lukefahr, and B. Andraka, Phys. Rev. Lett. **75**, 2023 (1995); D. E. MacLaughlin, O. O. Bernal, R. H. Heffner, G. J. Nieuwenhuys, M. S. Rose, J. E. Sonier, B. Andraka, R. Chau, and M. B. Maple, *ibid.* **87**, 066402 (2001); R. S. Hayano, Y. J. Uemura, J. Imazato, N. Nishida, T. Yamazaki, and R. Kubo, Phys. Rev. B **20**, 850 (1979).

[49] A. Keren, P. Mendels, I. A. Campbell, and J. Lord, Phys. Rev. Lett. **77**, 1386 (1996).

[50] A. Keren, G. Bazalitsky, I. Campbell, and J. S. Lord, Phys. Rev. B **64**, 054403 (2001).

[51] J. Spehling, M. Günther, C. Krellner, N. Yeche, H. Luetkens, C. Baines, C. Geibel, and H.-H. Klauss, Phys. Rev. B **85**, 140406(R) (2012).

[52] D. R. Grempel and M. J. Rozenberg, Phys. Rev. B **60**, 4702 (1999).

[53] H. Fujii, E. Ueda, Y. Uwatoko, and T. Shigeoka, J. Magn. Magn. Mater. **76-77**, 179 (1988).